



## Heat Transfer from a Hybrid Pulsating and Swirling Air Jet Impingement

Abhay Gudi<sup>1\*</sup>, Vijaykumar Hindasageri<sup>2</sup>

<sup>1</sup> Mechanical Engineering Department, VDIIT Haliyal, Haliyal 581329, India

<sup>2</sup> SME, Quest Global, Belagavi 590001, India

Corresponding Author Email: [abhayrg@klsvidit.edu.in](mailto:abhayrg@klsvidit.edu.in)

<https://doi.org/10.18280/ijht.400217>

**Received:** 19 March 2022

**Accepted:** 20 April 2022

### Keywords:

*Nusselt number, hybrid method, jet impingement, Reynolds number*

### ABSTRACT

With decrease in size of electronic equipment's, effective heat removal is a major challenge these days. Present work focuses on implementation of a novel hybrid method which helps attain heat transfer enhancement. An experimental investigation is carried out to study effect of pulse air jet on local heat transfer distribution of a flat surface. Effect of nozzle to plate distance ( $z/d = 2$  to  $6$ ), Reynolds number ( $5000$  to  $9000$ ), pulsating frequency ( $f = 0.07$  to  $2.03$  Hz) and Strouhal number ( $Sr = 6.7e-5$  to  $0.0029$ ) are studied with constant nozzle diameter. Thin foil technique is used to estimate local heat transfer characteristics using IR thermal infrared imaging technique. Nusselt number distribution is plotted for all the cases using information got from IR image. It is observed that at lower frequency rate and low Strouhal number heat, transfer rate is more effective. A novel hybrid method to improve heat transfer rate is introduced in this study using Pulse combined with swirl technique. This method involves introducing swirler of specified twist ratio into nozzle subjected to air pulse. Experiments show that this novel hybrid method improves heat transfer rate at all the above-mentioned conditions.

## 1. INTRODUCTION

Last three decades has seen lot of work on steady state air jet impingement heat transfer enhancement. Air jet impingement finds its application in many field that ranges from electronic cooling to glass and fabric processing [1-5]. With change in shape of electronic devices over period, it poses greater challenge in designing a device that effectively dissipates heat out of the system of electronic components. Jet cooling can be broadly classified into 4 types. This is summarized by Maghrabie [6] who brings out advantages of these methods that include Conventional jet cooling methodology, swirling jet cooling, Synthetic jet cooling and Pulsed air jet cooling.

Pulsating air jet, which is a type of active cooling method can be one such example that can be applied to achieve effective heat transfer. Kazem et al. [7] have shown experimentally that cooling performance of oscillating impinging jet is enhanced by increase in the frequency and amplitude of oscillation as well as decrease in nozzle to plate distance. Alimohammadi et al. [8] have shown experimentally and numerically that pulsating flows can produce additional enhancement in heat transfer when compared to steady flow for  $Re$  ranging between  $1300$  to  $2800$  with pulsating frequency of  $2$  Hz to  $65$  Hz and Strouhal number in the range of  $0.0012$  to  $0.084$ . Zulkifli and Sopian [9] have shown that the average pulsed jet Nusselt number was higher than the average steady jet Nusselt number for all values of frequencies due to the higher localised heat transfer of the pulsing jet. This was due to enhanced turbulence intensity due to pulsing the jet. The stagnation point heat transfer of the pulsed jet obtained was lower for the same frequency range due to the small turbulent intensity at this position. The pulsating frequency considered

was  $10$  to  $80$  Hz with Reynolds number ranging between  $16000$  to  $32000$ . Janetzke et al. [10] have shown 20% enhancement in cooling effectiveness is possible for Strouhal number as high as  $Sr = 0.82$  for high pulsating magnitude and of 15% cooling effectiveness for lower Strouhal numbers. Rakhsha et al. [11] have investigated effects of the pin on flow and heat transfer from pulsating jet impinging on a heated flat surface. They showed that presence of pin changes the coherent vortical of the flow structure at both upstream and downstream of the pins. At  $Re = 10000$  and  $H/d = 5$  the pulsed jet with frequencies of  $50$  Hz,  $80$  Hz, and  $100$  Hz increases the heat transfer from the pinned surface by 21%, 30%, and 36%, respectively, in comparison the steady jet. They have shown that the Nusselt number increases with increasing the pulse frequency and Reynolds number. Camci and Herr [12] have converted conventional jet into self-oscillating jet of frequency ranging from  $20$ - $100$  Hz and shown that there is significant increase in heat transfer ranging between 20-70% over conventional stationary jet because of oscillations. Reynolds number ranging between  $7500$ - $14000$  were studied in their work. Coulthard et al. [13] have shown that heat transfer enhancement is reduced with increase in pulse frequency. They used solenoid valve in their experiment to create pulse with frequency ranging between  $0.01$  Hz to  $0.75$  Hz. This work was more focused on inclined jet impingement with impingement angle of  $35^\circ$ . Lyu et al. [14] have shown experimentally that possibility of heat transfer enhancement is achieved under conditions  $Re \leq 7500$  and  $Sr(H/d) \geq 0.04$ ,  $Re \geq 17500$  and  $0.01 \leq Sr(H/d) \leq 0.03$ ;  $10 \text{ Hz} \leq f \leq 20 \text{ Hz}$  and  $Sr(H/d) \geq 0.04$ ;  $H/d \geq 6$ . Arik et al. [15] have done extensive experimental study on steady as well as pulsating jets. Synthetic jet which is one form of pulsating jets are used for studying the heat transfer in this work. They have shown that

synthetic jets provide higher cooling compared to steady jets at Reynolds number ranging between 1000-3000. Talapati et al. [16] have used synthetic jet to study local heat transfer characteristics on convex surface. Pulsating frequency studied range between 100-300 hz with jet to plate distance of  $z/d=1$  to 8. They have shown that pulsating frequency of 200 hz with jet to plate distance of  $z/d=2$  is more effective in obtaining higher heat transfer. Arik and Icoz [17] have developed closed form of correlation to predict the heat transfer coefficient as a function of jet geometry, position, and operating conditions for impinging flow based on experimental data. Their proposed correlation predicts synthetic jet impingement heat transfer within 25% accuracy for a wide range of operating conditions and geometrical variables.

From the literature survey done it is seen that for low pulse frequency ( $f < 2$  hz) & low Reynolds number ( $Re < 10000$ ) there is very limited work available. Current work considers pulse frequency range of 0.07 hz-2.03 hz with Reynolds number in range  $5000 \leq Re \leq 9500$ . A novel method is introduced in this work that showcases better heat transfer enhancement possibilities when compared to traditional pulse jet method.

Though above literature work covers heat transfer enhancement possibilities through pulse jet at wide range of Reynolds number, present work brings out possibility of further heat transfer enhancement. Wide objective of present work is outlined below:

- 1) Novel hybrid method which combines pulse+swirl is introduced to achieve better heat transfer enhancement.
- 2) Heat transfer enhancement for low Re flows ranging between 5000 to 9500.
- 3) Comparison of centerline Nusselt number values on

impingement surface with pulse jet and with pulse+swirl combination is explained for jet to plate distance  $z/d$  of 2 to 6.

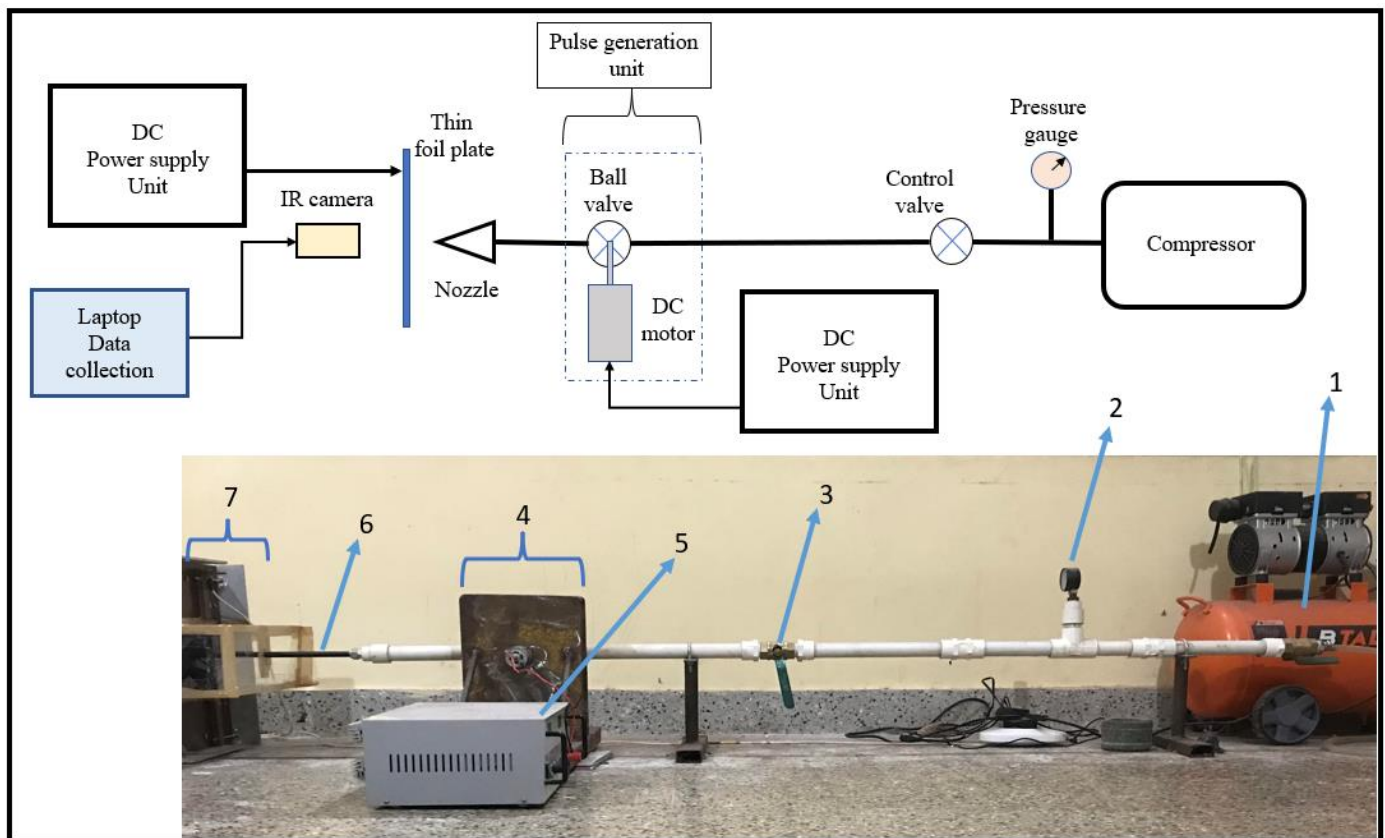
## 2. EXPERIMENTAL SETUP

Experimental setup details and schematic diagram of setup are shown in Figure 1. Air from the compressor is supplied to the test section through a UPVC pipe of diameter 1 inch. A nozzle of diameter 10 mm is attached at the other end of the pipe through which air impinges onto the target plate. Air flow rate is controlled by a control valve attached to the pipe. In current experimental method, air flow from the compressor passes through ball valve and then onto the nozzle. Ball valve shaft is attached to a high torque DC motor shaft through shaft coupler which is rotated through DC current supplier. This setup is shown in Figure 1 below.

Figure 2 shows pulse generation unit. This unit consists of a DC motor attached to valve through a couple. DC motor is rotated at specified RPM using power source connection which in turn rotates the vale thus, causing pulse generation inside the pipe. Frequency of pulse is varied by varying the speed of DC motor.

Air flow rate is measured using hot wire anemometer which is placed just at the area of jet exit. Figure 3 shows hot wire anemometer that is used in the experiment.

Heat transfer measurements are done using the thin foil technique. The target plate which is made of a thin stainless-steel foil (0.06 mm thick) of the dimension 215 mm x 145 mm attached to the copper bus bars. The target plate is heated by supplying electrical power to the bus bars through Variac (variable transformer).



1. Air Compressor; 2. Pressure Gauge; 3. Flow Control Valve; 4. Pulse generation unit; 5. DC power supply; 6. Nozzle; 7. Target plate setup implement

**Figure 1.** Schematic diagram of experimental setup

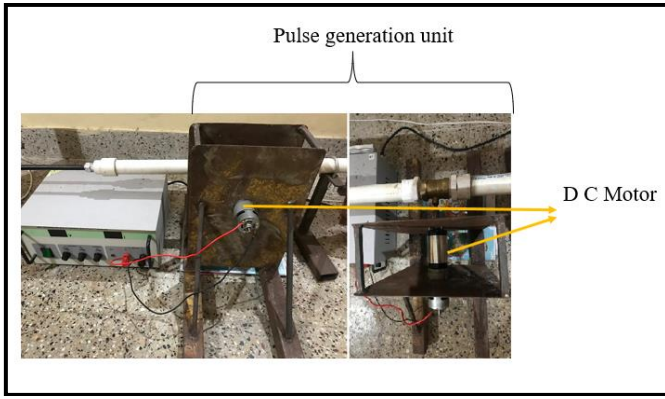


**Figure 2.** Pulse generation unit

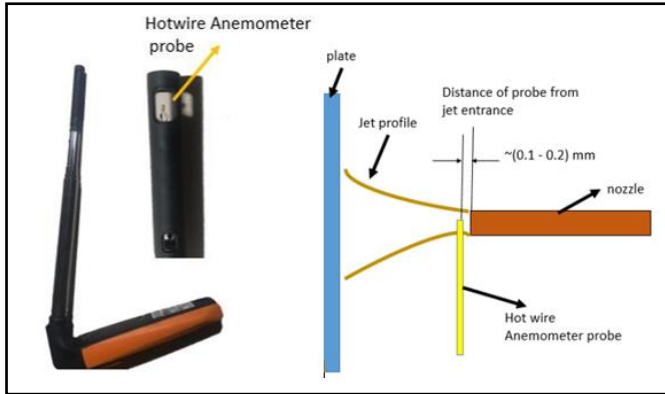


**Figure 3.** Testo anemometer schematic and probe position alignment during jet flow

The heat transfer distribution on the target plate is measured by capturing the thermal images obtained from an Infra-Red (IR) camera positioned on the back side of the target surface.

One dimensional energy balance across the heated plate shows negligible temperature difference across it. Hence, the local temperature measured on the back surface is the same as that on the impingement surface. The back side of the target surface is painted black using a thin coat of ‘Matte Finish Asian’ paint which provides high emissivity (0.99) surface. Infrared radiometry technique is used to measure local temperature from uniform heat flux surface which provides higher spatial resolution of temperature than thermocouples. ‘FLIR C3 Thermal Imaging’ infrared thermal camera is used to collect local temperature distribution with a resolution of about 360x240 screen resolution. Power is supplied from DC power source. The voltage across the target plate is measured by ‘Meco’ digital meter whose ranges and accuracies are of  $\pm 0.5\%$  V. Suitable voltage taps are provided in each of the bus bars. The jet air is allowed to impinge on the target plate with the heat input. The target plate allowed to acquire steady state temperature with the air jet and its temperature is measured by using thermal camera from the other side of the plate. Power loss from the exposed surface of the target plate due to natural convention and radiation is estimated experimentally. The procedure of heat loss estimation is explained in section below.

### 2.1 Estimation of heat loss

The temperature distribution on flat plate is obtained by images from IR thermal camera. Nusselt number is calculated as:

$$Nu = \frac{hd}{k} \quad (1)$$

$$h = q(\text{conv}) / (T_{\text{wall}} - T_{\text{ref}}) \quad (2)$$

$$q(\text{conv}) = q(w) - q(\text{loss}) \quad (3)$$

$$q(w) = VI/A \quad (4)$$

$$q(\text{loss}) = q(\text{rad}) + q(\text{nat}) \quad (5)$$

Heat loss from the plate is obtained by heating the plate at different time interval and measuring the wall temperature. A linear fit curve is obtained between heat loss and temperature difference between plate surface and ambient reference temperature. This is shown in Figure 4.

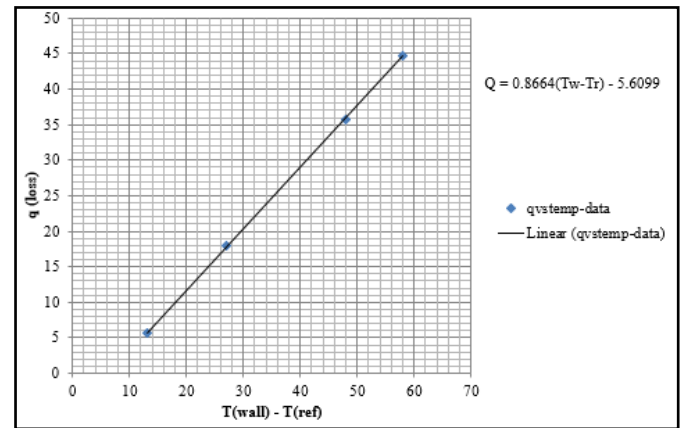


**Figure 4.** Heat loss linear fit curve

In present work, the temperature difference between the plate surface and jet was kept above 40°C that estimates a maximum uncertainty of not more than 2%. The heat flux uncertainty of plate is same as that of uncertainty of the power supplied. The uncertainties in the measurement of parameters by Moffat method [18] are mentioned in Table 1.

**Table 1.** Uncertainty of parameters

Parameters	Uncertainty (%)
d	0.1
f	0.1
z	0.1
t	0.33
$\Delta T$	1.6
V	0.12
I	0.4
Nu	3.01

### 2.2 A note on hot wire anemometer used in this experiment

‘Testo smart’ is the name of company that manufactures digital hotwire anemometer with an accuracy of  $\pm 0.5\%$  [19, 20].

Figure 3 shows the representation of hotwire anemometer with probe. As we know from literature [1-5] any impinging air jet is divided into four regions; a) initial mixing jet b) established jet c) deflection zone d) wall jet. Initial mixing jet region will have centerline velocity equal to jet exit velocity. Hence probe of hotwire anemometer is placed in such a manner that distance between nozzle jet exit and anemometer

probe is maintained as minimum as possible, thus measured velocity of air impinging out of jet is nozzle air velocity. Figure 3 shows distance of probe alignment with jet flow.

### 2.2.1 Characterization of variables used in pulse jet impingement

Previous section explained the method of measuring air flow using anemometer. In this section we take one example of flow and explain how air flow information got from anemometer is used to calculate nondimensional quantities like Re and St for various tests that are planned. In this paper, experimental results were carried out for Re varying between 9500 to 5000. Figure 5 shows velocity data for a sample case got from anemometer.

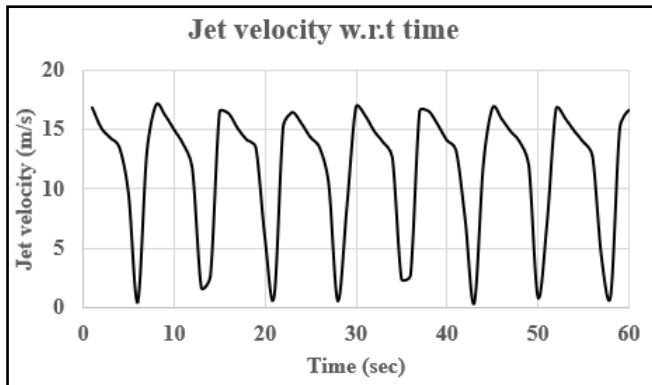


Figure 5. Jet Velocity measured at exit of Nozzle

Re and St are expressed as

$$Re = \frac{\rho U d}{\mu} \quad (6)$$

$$St = \frac{f d}{U} \quad (7)$$

In above equations U is the mean velocity got from anemometer, d is the hydraulic diameter of nozzle, f is the pulse frequency,  $\mu$  is dynamic viscosity of air and  $\rho$  is density of air.

Pulse frequency (f) is calculated as:

$$f = \frac{N}{60} \quad (8)$$

where, N = DC motor speed (rpm).

## 3. RESULTS AND DISCUSSION

### 3.1 Experimental validation

Experimental work is carried out to validate study conducted by Alimohammadi et al. [8]. Figure 6 shows results of centerline Nu data validation for the work mentioned.

Experimental results match very well with results got by Alimohammadi et al. [8] for  $f=2\text{hz}$ ;  $Re=1300$ ;  $St=0.0012$ ;  $z/d=1$ . Stagnation point Nu vary by 2% w.r.t results of Alimohammadi et al. [8]. In coming sections, we discuss the results of proposed experiments for pulse jet impingement.

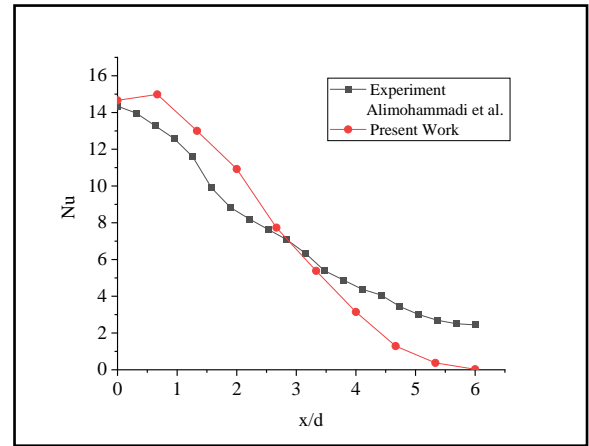


Figure 6. Centerline Nu distribution

### 3.2 Effect of pulsating frequency

Air jet Pulse frequency was varied between 0.07 Hz to 2.033 Hz. Plate to jet distance ( $z/d$ ) was varied between 2 to 6 for all mentioned frequency conditions. Figure 7 shows centerline distribution of Nu for pulse frequency mentioned above.

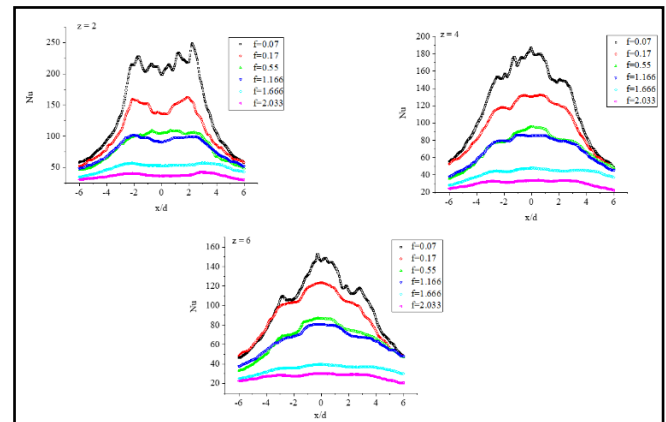


Figure 7. Centerline Nu distribution

- Following observations can be made from the above study:
- Heat transfer is more effective at lower pulse frequency ( $f=0.07\text{ hz}$ ) when compared to higher pulse rate ( $f=2.03\text{ hz}$ ).
  - Higher heat transfer effectiveness is seen at  $z/d=2$  when compared to  $z/d=6$ .

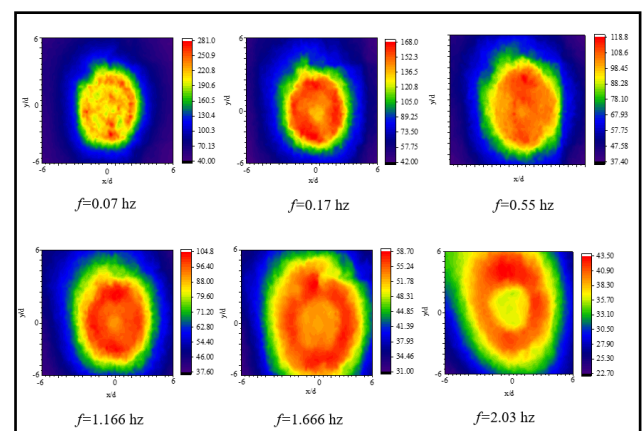


Figure 8. Contours of Nu distribution on target plate for different pulse frequencies at  $z/d=2$

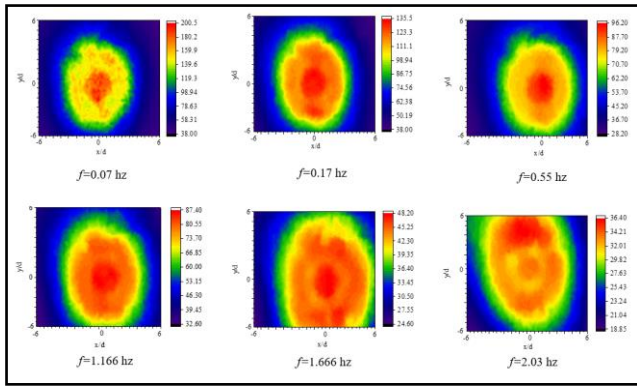


Figure 9. Contours of Nu distribution on target plate for different pulse frequencies at  $z/d=4$

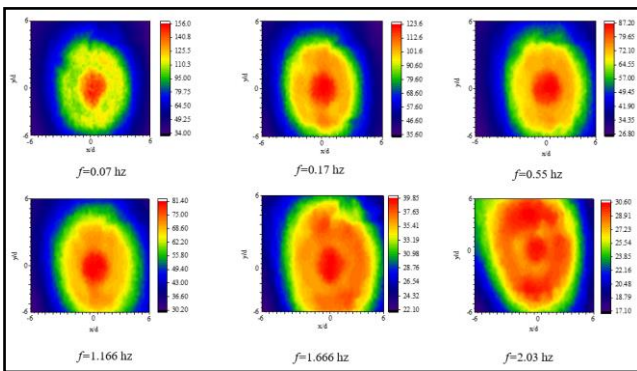


Figure 10. Contours of Nu distribution on target plate for different pulse frequencies at  $z/d=6$

Figures 8-10 below show Nu distribution on target plate for the  $z/d=2,4,6$  with pulse frequency varying between 0.07 to 2.03 hz.

We observe that, with increase in pulse frequency, jet spread increases which decreases the heat transfer effectiveness. Hence, we see decrease in centerline Nu distribution on the plate.

### 3.3 Effect of jet to plate distance

Effect of jet to plate distance was studied on to understand this effect on heat transfer enhancement. Distance  $z/d$  was varied from 2 to 6 by keeping pulse frequency ( $f$ ), Reynolds number ( $Re$ ) and Strouhal number ( $St$ ) constant. Figure 11 shows centerline distribution of Nu on impingement plate for varying jet to plate distances.

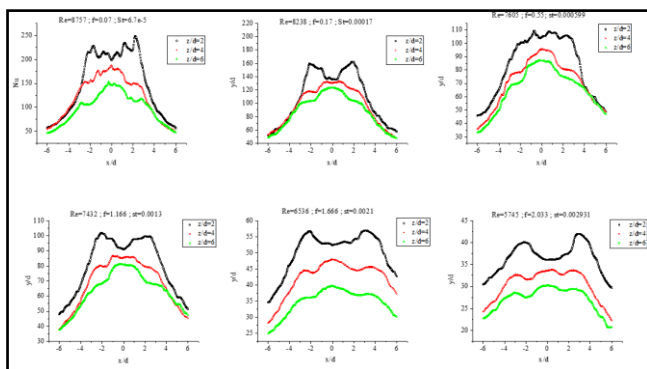


Figure 11. Centerline Nu distribution for different jet to plate distances

Experimental results show that, with increase in jet to plate distance, heat transfer effectiveness decreases regardless of pulse frequency and Reynolds number.

Figure 12 shows the effect of jet to plate distance on Stagnation Nu for different pulse frequencies that are discussed above.

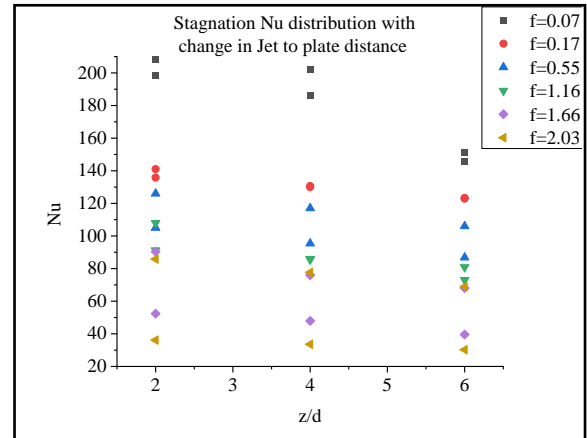


Figure 12. Stagnation Nu variation w.r.t Jet to plate distance at different pulse frequencies

Following observations can be made from Figure 12.

- There is a decrease in stagnation Nu with increase in jet to plate distance for constant pulse frequency ranges.
- Decrease in pulse frequencies at fixed jet to plate distance indicate that Reynolds number of flow is decreasing which results in lesser heat transfer. Hence measured stagnation number show decreasing pattern regardless of jet to plate distance.

## 4. PROPOSED NOVEL HYBRID METHOD TO INCREASE HEAT TRANSFER EFFECTIVENESS

There have been extensive studies done on swirl jets [6] which indicate that heat transfer enhancement is possible by introducing swirler in the air flow passage. With swirlers, it is seen that heat transfer enhancement is possible for low Reynolds number ( $Re \leq 5000$ ) cases. This has led to authors to introduce a novel hybrid method of enhancing heat transfer rate.

In this method, we introduce swirler of twist ratio ( $T.R=2.5$ ) into the nozzle subjected to pulse flow. Figure 13 shows swirler with twist ratio of 2.5 used in this experiment.

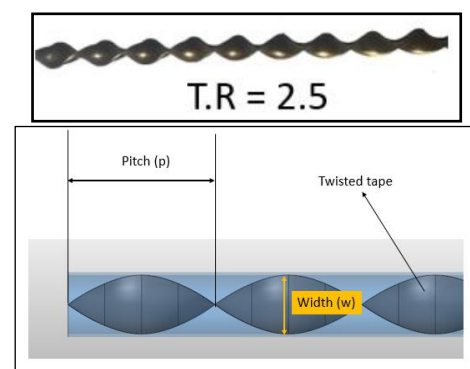


Figure 13. Swirler with  $T.R=2.5$  used in experiment

Twist ratio is defined as

$$T.R = \frac{\text{Pitch of swirler}}{\text{width of swirler}}$$

Experimental studies conducted with pulse jet are further repeated with this approach. Results got are discussed in below section.

#### 4.1 Effect of pulse frequency

Figures 14-16 show centerline Nu results of Pulse+swirl combination for pulse frequencies in range of 0.07 hz to 2.03 hz.

It is evident from the results that Pulse+swirl combination mechanism results provide higher heat transfer compared to cases of pure pulse air jet impingement.

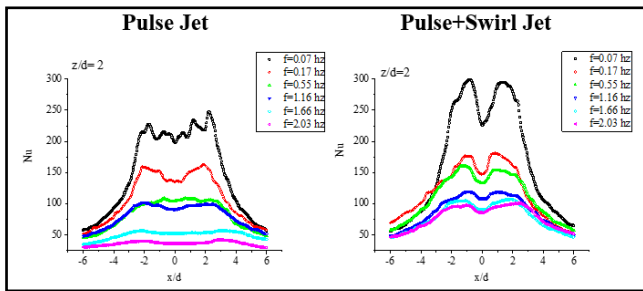


Figure 14. Centerline Nu comparison of Swirl+Pulse with Pulse air jet at z/d=2

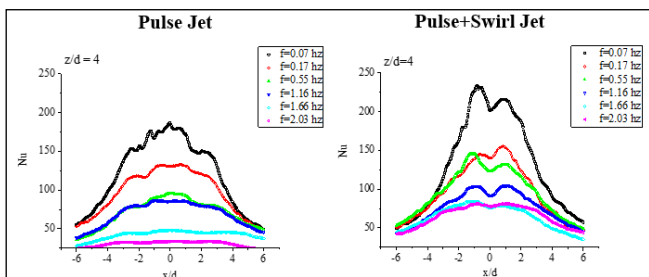


Figure 15. Centerline Nu comparison of Swirl+Pulse with Pulse air jet at z/d=4

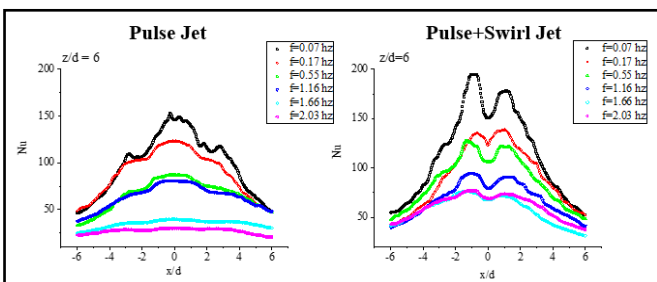


Figure 16. Centerline Nu comparison of Swirl+Pulse with Pulse air jet at z/d=6

Figures 17-19 below show contour plot Nu distribution on target plate for the z/d=2,4,6 with pulse+swirl mechanism with frequency varying between 0.07 to 2.03 hz.

From above contour plots it is evident that with increase in jet to plate distance and increase in pulse frequency, jet spread

increases and there is decrease in heat transfer.

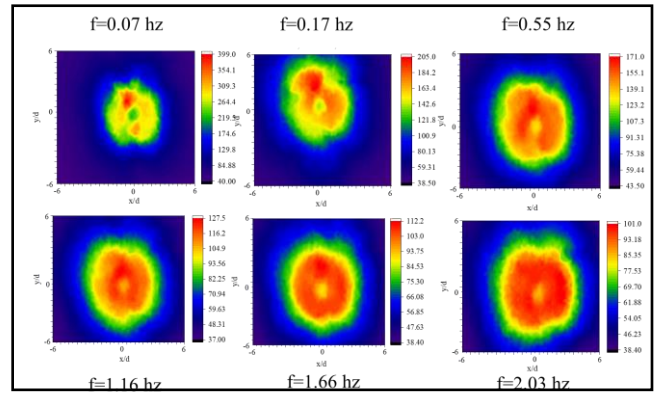


Figure 17. Contours of Nu distribution on target plate for different pulse frequencies at z/d=2

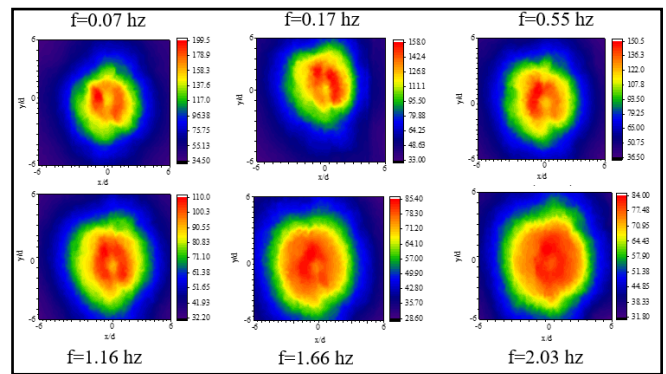


Figure 18. Contours of Nu distribution on target plate for different pulse frequencies at z/d=4

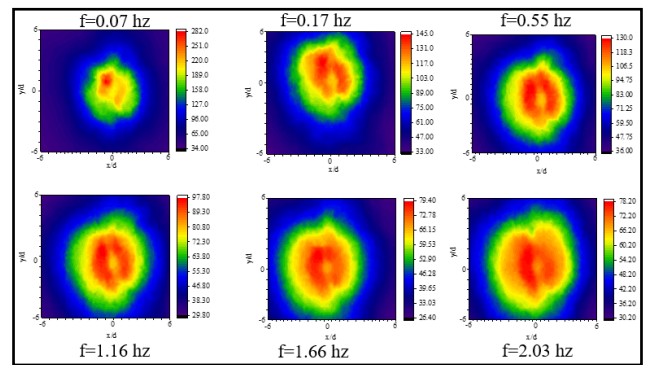
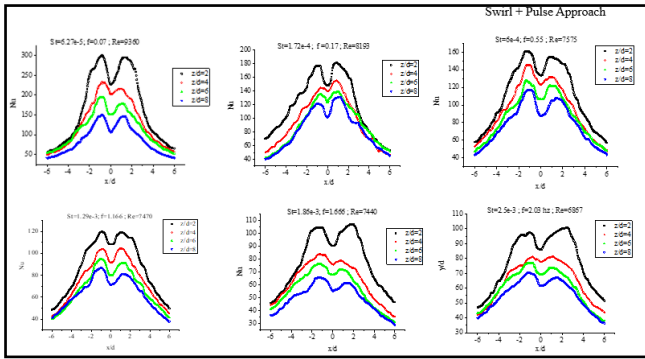


Figure 19. Contours of Nu distribution on target plate for different pulse frequencies at z/d=6

#### 4.2 Effect of Jet to plate distance

This section showcases effectiveness study of Pulse+swirl mechanism considering jet to plate distance. Here jet to plate distance used was  $2 < z/d < 8$ . Figure 20 shows centerline Nu distribution on plate.

This study too depicts same behavior of centerline Nu as in case of pure pulse study. However, we observe that heat transfer effectiveness is more in this case and due to presence of swirler, there is a drop in heat transfer at the stagnation region. We also observe that stagnation Nu decreases with increase in jet to plate distance for all cases. This is shown in Figure 21.



**Figure 20.** Centerline Nu distribution for different jet to plate distances

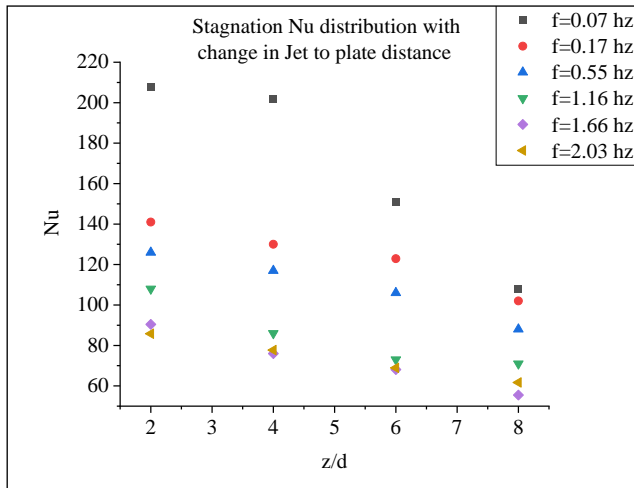


**Figure 21.** Stagnation Nu variation w.r.t Jet to plate distance at different pulse frequencies

## 5. CONCLUSION

The local heat characteristics of pulsating air jet impinging on a plate surface is studied experimentally by using thin foil technique. Pulse frequency used for experiment was in the range  $f=0.07$  to  $2.03$  Hz. Jet to plate distance ( $z/d=2$  to  $6$ ) with jet nozzle diameter of  $11$  mm was used. Results obtained from this study are mentioned below.

- With increase in air jet pulse frequency ( $f=0.07$  to  $2.03$  Hz) local heat transfer decreases. At jet to plate distance of  $z/d=2$  and with  $f=0.07$  Hz it is seen that heat transfer rate is lesser at stagnation region. This is due to high momentum of pulsating jet on plate. As jet to plate distance is increased, heat transfer rate at stagnation region increases due to decreases in pulse momentum.
- Local Nu decreases with increase in jet to plate distance ( $z/d=2$  to  $6$ ) for all pulse frequency ranges. Jet to plate distance of  $z/d=2$  is most effective to achieve maximum heat transfer rate regardless of any pulse frequencies.

The local heat transfer characteristics is studied for proposed novel method in which pulse air jet is combined with swirl generator of twist ratio  $2.5$ . Above mentioned experiments are repeated for this method for conditions of pulse frequency  $f=0.07$  to  $2.03$  Hz and jet to plate distance of  $z/d=2$  to  $6$ . Results obtained are mentioned below.

- As pulse frequency increases ( $f=0.07$  to  $2.03$  Hz), local

heat transfer decreases.

- It is observed that for all jet to plate distances ( $z/d=2$  to  $8$ ), heat transfer is maximum away from stagnation region. This is due to the presence of swirler which caused swirling effect or high momentum away from stagnation region. Thus, heat transfer is lesser at stagnation point.
- Local Nu decreases with increase in jet to plate distance ( $z/d=2$  to  $6$ ) for all the mentioned frequency ranges.
- Very similar to pure pulse jet impingement cases, in this method too we observe that jet to plate distance of  $z/d=2$  is more effective in achieving maximum heat transfer.

Limitations and future research directions of present work are listed below:

- $1.05$  Hp compressor was used in present work which limits the total amount of air flow. As we were mostly interested in low Reynolds number study,  $1.05$  Hp compressor was enough to fulfill our air flow requirement. Future directions can be one to include higher Hp compressor which would help increase the flow rate inside the pipe eventually increase the Reynolds number.
- There is future scope of conducting a numerical study to achieve correlations of present work and propose a higher Reynolds number pulse air jet impingement work.
- Flow control valve used in present work have a limitation of flow that can be reduced up to  $Re \sim 1500$ . Present valves can be replaced by rotary valves which could help reduce the flow further such that laminar air jet impingement can also be included as a future scope.

## REFERENCES

- [1] Kattim V., Prabhu, S.V. (2008). Experimental study and theoretical analysis of local heat transfer distribution between smooth flat surface and impinging air jet from a circular straight pipe nozzle. *Int J Heat Mass Transf.*, 51(17-18): 4480-4495. <https://doi.org/10.1016/j.ijheatmasstransfer.2007.12.024>
- [2] Katti, V., Nagesh, Y., Prabhu, S.V. (2011). Local heat transfer distribution between smooth flat surface and impinging air jet from a circular nozzle at low Reynolds numbers. *Heat Mass Transf.*, 47: 237-244. <https://doi.org/10.1007/s00231-010-0716-1>
- [3] Gulati, P., Katti, V., Prabhu, S.V. (2009). Influence of the shape of the nozzle on local heat transfer distribution between smooth flat surface and impinging air jet. *Int. J. Therm. Sci.*, 48(3): 602-617. <https://doi.org/10.1016/j.ijthermalsci.2008.05.002>
- [4] Martin, H. (1977). Heat and mass transfer between impinging gas jets and solid surfaces. *Advances in Heat Transfer*, 13: 1-60. [https://doi.org/10.1016/S0065-2717\(08\)70221-1](https://doi.org/10.1016/S0065-2717(08)70221-1)
- [5] Lytle D, Webb, B.W. (1994). Air jet impingement heat transfer at low nozzle-plate spacing's. *Int. J. Heat Mass Transf.*, 37: 1687-1697.
- [6] Maghrabie, H.M. (2021). Heat transfer intensification of jet impingement using exciting jets – A comprehensive

- review. *Renewable and Sustainable Energy Reviews*, 139: 110684. <https://doi.org/10.1016/j.rser.2020.110684>
- [7] Esmailpour, K., Hosseinalipour, M., Bozorgmehr, B., Mujumdar, A.S. (2015). A Numerical study of heat transfer in a turbulent pulsating impinging jet. *Canadian Journal of Chemical Engineering*, 93(5): 959-969. <https://doi.org/10.1002/cjce.22169>
- [8] Alimohammadi, S., Dinneen, P., Persoons, T., Murray, D.B. (2014). Thermal management using pulsating jet cooling technology. *Journal of Physics: Conference Series*, 525: 01201. <https://doi.org/10.1088/1742-6596/525/1/012011>
- [9] Zulkifli1, R., Sopian, K. (2006). Pulsating circular air jet impingement heat transfer. *Journal - The Institution of Engineers, Malaysia*, 67(3).
- [10] Janetzke, T., Nitsche, W., Täge, J. (2008). Experimental investigations of flow field and heat transfer characteristics due to periodically pulsating impinging air jets. *Heat Mass Transfer*, 45: 193-206. <https://doi.org/10.1007/s00231-008-0410-8>
- [11] Rakhsha, S., Zargarabadi, M.R., Saedodin, S. (2019). Experimental and numerical study of flow and heat transfer from a pulsed jet impinging on a pinned surface. *Experimental Heat Transfer*, 34(4): 376-391. <https://doi.org/10.1080/08916152.2020.1755388>
- [12] Camci, C., Herr, F. (2002). Forced convection heat transfer enhancement using a self-oscillating impinging planar jet. *Journal of Heat Transfer*, 124(4): 770-782. <https://doi.org/10.1115/1.1471521>
- [13] Coulthard, S.M., Volino, R.J., Flack, K.A. (2007). Effect of jet pulsing on film cooling—Part II: Heat transfer results. *Journal of Turbomachinery*, 129(2): 247-257. <https://doi.org/10.1115/1.2437230>
- [14] Lyu, Y.W., Zhang, J.Z., Shan, Y., Tan, X.M. (2018). The experimental investigation of impinging heat transfer of pulsation jet on the flat plate. *Journal of Heat Transfer*, 140(12): 122202. <https://doi.org/10.1115/1.4041183>
- [15] Arik, M., Sharma, R., Lustbader, J., He, X. (2013). Steady and unsteady air impingement heat transfer for electronics cooling applications. *Journal of Heat Transfer*, 135(11): 111009. <https://doi.org/10.1115/1.4024614>
- [16] Talapati, R.J., Katti, V.V., Hiremath, N.S. (2021). Local heat transfer characteristics of synthetic air jet impinging on a smooth convex surface. *International Journal of Thermal Sciences*, 170: 107143. <https://doi.org/10.1016/j.ijthermalsci.2021.107143>
- [17] Arik, M., Icoz, T. (2012). Predicting Heat Transfer from Unsteady Synthetic Jets. *Journal of Heat Transfer*, 134(8): 081901. <https://doi.org/10.1115/1.4005740>
- [18] Moffat, R.J. (1988). Describing the uncertainties in experimental results. *Exp. Therm. Fluid Sci.*, 1(1): 3-17. [https://doi.org/10.1016/0894-1777\(88\)90043-X](https://doi.org/10.1016/0894-1777(88)90043-X)
- [19] Yang, D.Z., Xie, J., Wang, J.F., Shu, Z.T. (2019). Effect of jet arrangement and jet height on flow characteristics of air impingement. *Journal of Chemical Engineering of Japan*, 52(2): 179-184. <https://doi.org/10.1252/jcej.18we007>
- [20] Cano, J.S., Cordova, G.D., Narvaez, C., Segura, L., Carrion, L. (2019). Experimental study of the incidence of changing a synthetic jet orifice in heat transfer using a Taguchi method approach. *Journal of Thermal Science and Engineering Applications*, 11(3): 031011. <https://doi.org/10.1115/1.4042351>

## NOMENCLATURE

$A$	Surface area of plate (m <sup>2</sup> )
$D$	Diameter of jet hole (m)
$h$	Heat transfer coefficient (W/m <sup>2</sup> K)
$k$	Thermal conductivity of air (W/m k)
$Nu$	Nusselt number
$Re$	Reynolds number
$Sr$	Strouhal number
$f$	Pulse frequency (hz)
$\mu$	Dynamic Viscosity
$\rho$	Density
$t$	Thickness
$z/d$	Jet exit to plate distance
$T_{wall}$	Surface temperature of plate
$T_{ref}$	Reference temperature
$q_{(conv)}$	Convection heat loss
$q_{(rad)}$	Radiative heat loss
$q_{(w)}$	Surface heat loss
$q_{(loss)}$	Sum of heat loss due to radiation and natural convection
$N$	DC Motor speed
$V$	Voltage (Volts)
$I$	Current (Amps)
$p$	Swirler pitch
$w$	Swirler width